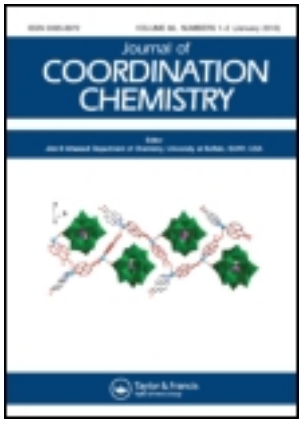

Journal of Coordination Chemistry
Publication details, including instructions for authors and subscription information:
http://www.tandfonline.com/loi/gcoo20

Positional isomeric and N-donor auxiliary chelating ligand effect on engineering crystalline architectures of four lead(II) complexes with diverse fluorescent properties

Wei Liang [a], Zhaoyin Zhong [a], Zi-Cai Pan [a], Qing-Hua Meng [b], Ye Deng [a] & Kou-Lin Zhang [a]

[a] Key Laboratory of Environmental Material and Environmental Engineering of Jiangsu Province, College of Chemistry and Chemical Engineering, Yangzhou University, Yangzhou, P.R. China

[b] College of Chemistry and Chemical Engineering, Jiangsu Normal University, Xuzhou, P.R. China

Accepted author version posted online: 14 Jun 2013.Published online: 16 Jul 2013.

To cite this article: Wei Liang, Zhaoyin Zhong, Zi-Cai Pan, Qing-Hua Meng, Ye Deng & Kou-Lin Zhang (2013) Positional isomeric and N-donor auxiliary chelating ligand effect on engineering crystalline architectures of four lead(II) complexes with diverse fluorescent properties, Journal of Coordination Chemistry, 66:16, 2802-2820, DOI: 10.1080/00958972.2013.815747

To link to this article: http://dx.doi.org/10.1080/00958972.2013.815747

Journal of Coordination Chemistry, 2013
Vol. 66, No. 16, 2802–2820, http://dx.doi.org/10.1080/00958972.2013.815747

Positional isomeric and N-donor auxiliary chelating ligand effect on engineering crystalline architectures of four lead(II) complexes with diverse fluorescent properties

WEI LIANG†, ZHAOYIN ZHONG†, ZI-CAI PAN†, QING-HUA MENG‡, YE DENG† and KOU-LIN ZHANG*†

†Key Laboratory of Environmental Material and Environmental Engineering of Jiangsu Province, College of Chemistry and Chemical Engineering, Yangzhou University, Yangzhou, P.R. China

‡College of Chemistry and Chemical Engineering, Jiangsu Normal University, Xuzhou, P.R. China

(*Received 2 December 2012; in final form 10 May 2013*)

This work presents an investigation on the positions of the substituent and N-donor auxiliary chelating ligand (bipy/phen) effect on engineering of crystalline architectures of four Pb(II) complexes with a pair of methyl-substituted 3-sulfobenzoic isomers: [Pb(4-msba)(phen)(H_2O)] (**1**), [Pb(4-msba)(bipy)(H_2O)]·H_2O (**2**), [Pb(5-msba)(phen)$_2$]·$9H_2O$ (**3**), and [Pb$_2$(5-msba)$_2$(bipy)$_2$(H_2O)$_2$] (**4**) (4/5-msba = 4/5-methyl-3-sulfobenzoate, phen = 1,10-phenanthroline and bipy = 2,2′-bipyridine). The lead(II) ions exhibit hemidirected geometry in **1–4**. The positions of the methyl as well as the auxiliary chelating ligands influence coordination modes of the sulfonates and thus determine the architectures. As the position of methyl in aromatic ring changes from 4 to 5, the structures change from 2-D sheet-like compounds for **1** and **2** to 0-D dimeric species for **3** and **4**. A water cluster $(H_2O)_{18}$ exists in **3**, which further assembles into a water tape with a new pattern T4(3)4(3)10(3)A4. Complex **3** loses crystallinity rapidly in the open air and turns into [Pb(5-msba)(phen)$_2$]·$2H_2O$ (**3A**). Thermal stabilities and solid state fluorescent properties of **1**, **2**, **3A**, and **4** have been studied.

Keywords: Positional isomeric effect; Lead(II) complexes; Crystal structures; Characterization; Fluorescence spectra

1. Introduction

Metal–organic frameworks (MOFs) have versatile coordination motifs and potential applications in many fields [1–8]. The construction of crystalline architectures depends on the combination of several factors, such as ligands, the coordination environment of metal nodes, solvents, counter ions, and non-covalent interactions [9–13]. A better understanding of how these considerations influence crystal packing is a prerequisite for improving the ability to rationally design and synthesize supramolecular functional materials. Organic ligands are easily modified with different substituents and as a result coordination modes can be influenced [14–16]. Therefore, the prospect of tuning the architectures and

*Corresponding author. Email: klzhang@yzu.edu.cn

properties of MOFs through modification of organic ligands provides an impetus for further research on metal–organic supramolecular complexes [17, 18].

Design and control over coordination compounds are mainly focused on incorporation of *s*-, *d*-, and *f*-block metal ions as coordination centers, whereas less attention has been paid to *p*-block metals despite important applications in electroluminescent devices and fluorescent sensors [19, 20]. Thus, Pb(II) complexes remain less developed. Compared with transition metal ions, Pb(II) has large ionic radius, variable coordination numbers, and diverse coordination geometries. Pb(II) also has a tendency to provide a stable framework structure and potential in construction of functional materials [21–25]. Particularly, Pb(II) possesses evidence of coordination sphere distortions as a consequence of the presence of a $6s^2$ lone pair. The unique characteristic of Pb(II) causes interest in coordination chemistry, photochemistry, and nanomaterials [26–31]. Fluorescence in Pb(II) complexes may partly be attributed to ligation of ligand, which further enhances the rigidity of the ligand and reduces the loss of energy through a radiationless pathway. The coordination chemistry of Pb(II) has been investigated regarding the valence shell lone electron pair [32, 33]. The Pb(II) coordination is classified as "holodirected" when the bonds to ligands are directed throughout the surface of an encompassing sphere, and as "hemidirected" in cases where the bonds are directed throughout only a part of the coordination sphere, leaving a gap in the distribution of bonds to ligands. However, structural studies have been limited owing to the lack of suitable Pb(II) compounds. Only a few Pb(II) carboxylate-bridged complexes with layered or 3D network structures have been reported [28, 34–40].

Systematic studies on the influence of the substituent in the aromatic ring on structures of MOFs are rare [41, 15, 16] and there remain no systematic studies about the influence of the positions of substituent in the aromatic ring on the structures of Pb(II) supramolecular complexes. Organosulfonates have been extensively used to construct MOFs by Shimizu and coworkers [42–45]. To understand the Pb(II) chemistry with polyfunctional ligands, 5-sulfosalicylic acid has been selected for preparing Pb(II) complexes [26, 27]. However, there are still no complexes reported with methyl-substituted 3-sulfobenzoate ligands. 1,10-Phenanthroline (phen) and 2,2′-bipyridine (bipy) have been widely used to build supramolecular architectures due to great potential to form π…π stacking interactions.

Here, we select two isomeric methyl-substituted 3-sulfobenzoic acids, H_2(4-msba) and H_2(5-msba), as spacers and bipy/phen as auxiliary chelating ligands to assemble with Pb(II) (4/5-msba = 4/5-methyl-3-sulfobenzoate) (scheme 1). We report the syntheses and characterization of four Pb(II) complexes, [Pb(4-msba)(phen)(H_2O)] (**1**), [Pb(4-msba)(bipy)]·H_2O (**2**), [Pb(5-msba)(phen)$_2$]·9H_2O (**3**), and [Pb_2(5-msba)$_2$(bipy)$_2$(H_2O)$_2$] (**4**). The water cluster $(H_2O)_{18}$ is found in **3**, which further assembles into a water tape with a new tape pattern T4(3)4(3)10(3)A4. Complex **3** loses crystallinity rapidly in the open air and turns into [Pb(5-msba)(phen)$_2$]·2H_2O (**3A**). We demonstrate the effects of the positions of the methyl group and N-donor auxiliary chelating ligands on the architectures of Pb(II) supramolecular complexes. Solid state fluorescent properties and thermal stabilities have also been explored.

2. Experimental

2.1. *Materials and measurements*

All reagents except for 4-methyl-3-sulfobenzoic acid and 5-methyl-3-sulfobenzoic acid were purchased commercially. Elemental analyses (C, H, and N) were carried out on a 240

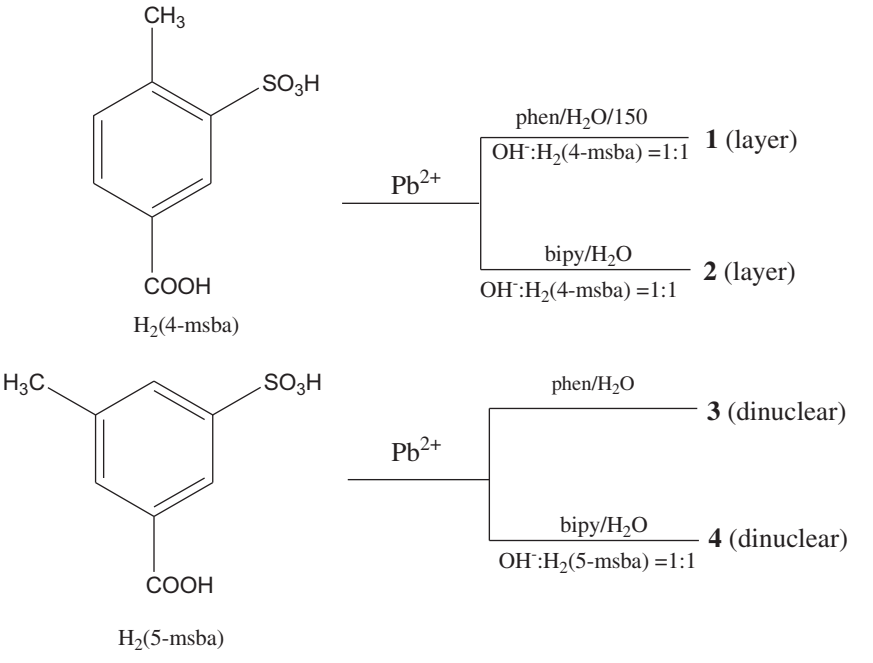

Scheme 1. Simplified representation of the synthesis of four Pb(II) complexes **1**-**4**.

C Elemental analyzer. FT-IR spectra (4000–400 cm^{-1}) were recorded from KBr pellets in a Magna 750 FT-IR spectrophotometer. Solid state fluorescence spectra were recorded using an F-4500 fluorescence spectrophotometer (Hitachi) equipped with a phosphorescence device. Both the excitation and emission pass width are 5.0 nm.

2.2. *Synthesis of ligands and complexes*

2.2.1. H_2(4-msba) and H_2(5-msba). The two isomers, H_2(4-msba) and H_2(5-msba), were synthesized in a similar way. Sulfuric acid (fuming 50%, 10 mL) was added slowly to 4/5-methylbenzoic acid (10 g) in a flask. The solution was refluxed for 4 h at 160–170 °C and then poured into an aqueous solution of NaCl (10 g) in water (100 mL). The mixture was filtered immediately. White powders were obtained when the solution was cooled to room temperature. The products were recrystallized with distilled water (50 mL): one time for H_2(4-msba) and three times for H_2(5-msba) (yield: 71, 52% based on 4/5-methylbenzoic acid), respectively. Anal. Calcd (%) for $C_8H_8O_5S$: C, 52.18; H, 4.38. Found: C, 51.97; H, 4.34 for H_2(4-msba) and C, 52.03; H, 4.42 for H_2(5-msba). ^{1}H NMR (400 MHz, DMSO-d_6). For 4-msba: δ 12.81 (1H, s, br), 8.30 (1H, s), 7.72 (1H, d), 7.27 (1H, d), 3.36 (1H, s, br), 2.50 (3H, s); For 5-msba: δ 12.96 (1H, s, br), 8.02 (1H, s), 7.77 (1H, s), 7.73 (1H, s), 3.45 (1H, s, br), 2.51 (3H, s).

2.2.2. [Pb(phen)(4-msba)(H_2O)] (1). A mixture of H_2(4-msba) (0.022 g, 0.1 mmol) and NaOH (0.004 g, 0.1 mmol) was dissolved in water (6 mL), and then a mixture of $Pb(NO_3)_2$ (0.033 g, 0.1 mmol) and phen (0.020 g, 0.1 mmol) in water (6 mL) was added while

stirring. Then, the mixture was loaded in a 25 mL Teflon-lined stainless steel vessel and heated at 155 °C for three days. Pale yellow crystals were obtained [yield: 61% based on H_2(4-msba)]. Anal. Calcd (%) for $C_{20}H_{16}N_2O_6PbS$: C, 38.77; H, 2.60; N, 4.52. Found: C, 38.91; H, 2.64; N, 4.63.

2.2.3. [Pb(bipy)(4-msba)(H_2O)]·H_2O (2). An aqueous solution of H_2(4-msba) (0.022 g, 0.1 mmol) in water (5 mL) was added to a mixture of $Pb(NO_3)_2$ (0.033 g, 0.1 mmol) and bipy (0.016 g, 0.1 mmol) in water (13 mL) while stirring. Then, NaOH (0.004 g, 0.1 mmol) was added to this solution and filtered. Pale yellow crystals were formed after the filtrate was kept under open air for several days [yield: 64% based on H_2(4-msba)]. Anal. Calcd (%) for $C_{18}H_{18}N_2O_7PbS$: C, 35.23; H, 2.96; N, 4.57. Found: C, 35.40; H, 3.04; N, 4.67.

2.2.4. [Pb(5-msba)(phen)$_2$]·9H_2O (3). A mixture of phen (0.020 g, 0.1 mmol) in water (7 mL) and $Pb(NO_3)_2$ (0.033 g, 0.1 mmol) in water (4 mL) was added to an aqueous solution of H_2(5-msba) (0.022 g, 0.1 mmol) in water (8 mL) with stirring. The filtration was kept under open air for one week and pale yellow block crystals were obtained.

Complex **3** loses crystallinity rapidly and turns into the pale yellow powder [Pb(5-msba)(phen)$_2$]·2H_2O (**3A**) [yield: 51% based on H_2(5-msba)]. Anal. Calcd (%) for $C_{32}H_{26}N_4O_7PbS$: C, 46.99; H, 3.20; N, 6.85. Found: C, 47.23; H, 3.29; N, 6.97.

2.2.5. [Pb$_2$(5-msba)$_2$(bipy)$_2$(H_2O)$_2$] (4). A mixture of $Pb(NO_3)_2$ (0.067 g, 0.2 mmol) and bipy (0.062 g, 0.4 mmol) in water (9 mL) was added to a mixture of H_2(5-msba) (0.043 g, 0.2 mmol) and NaOH (0.004 g, 0.1 mmol) in water (14 mL). The filtrate was kept at ambient temperature for several days and white block crystals were obtained [yield: 70% based on H_2(5-msba)]. Anal. Calcd (%) for $C_{36}H_{32}N_4O_{12}Pb_2S_2$: C, 36.30; H, 2.70; N, 4.70. Found: C, 36.51; H, 2.81; N, 4.78.

2.3. *X-ray single-crystal structure determination*

Crystallographic data were collected with a Siemens SMART CCD diffractometer using graphite-monochromated (Mo-Kα) radiation ($\lambda = 0.71073$ Å), ψ and ω scans mode. The structures were solved by direct methods and refined by full-matrix least-squares on F^2 using SHELXL-97 [45]. Intensity data were corrected for Lorenz and polarization effects and a multi-scan absorption correction was performed. The positions of C-bound hydrogens were generated geometrically. The hydrogens of water except **3** were first located in difference Fourier maps and then fixed. Hydrogens of water molecules in **3** cannot be added satisfactory, although great efforts have been made. All non-hydrogen atoms were refined anisotropically. The contribution of the hydrogen atoms was included in the structure factor calculations. Details of crystallographic data are listed in table 1.

3. Results and discussion

3.1. *Synthesis of the complexes*

The hydrothermal method was used in the synthesis of **1**, since single crystals suitable for X-ray analysis could not be obtained under ambient conditions. Complexes **2–4** were

Table 1. Crystallographic and structure refinement data for **1–4**.

	1	**2**
Empirical formula	$C_{20}H_{16}N_2O_6PbS$	$C_{18}H_{18}N_2O_7PbS$
Formula weight	619.60	613.59
Temperature (K)	293(2)	293(2)
Wavelength (Å)	0.71073	0.71073
Crystal system	Monoclinic	Monoclinic
Space group	$P2_1/n$	$P2_1/n$
a (Å)	9.5705(5)	9.4290(5)
b (Å)	19.0315(10)	19.3164(11)
c (Å)	11.3527(6)	11.1628(6)
α (°)	90	90
β (°)	91.9410(10)	91.3000(10)
γ (°)	90	90
Volume [Å^3]	2066.61(19)	2032.61(19)
Z	4	4
D_{Calcd} [Mg/m^3]	1.991	2.005
Absorption coeff. [mm^{-1}]	8.305	8.446
F (000)	1184	1176
θ Range for data collection (°)	2.09–27.49	2.40–27.50
Index ranges	$-12 \leqslant h \leqslant 12$ $-24 \leqslant k \leqslant 24$ $-14 \leqslant l \leqslant 14$	$-12 \leqslant h \leqslant 11$ $-25 \leqslant k \leqslant 25$ $-14 \leqslant l \leqslant 12$
Reflections collected	19,953	17,404
Unique (R_{int})	4748 [R(int) = 0.0285]	4623 [R(int) = 0.0260]
Completeness to $\theta = 27.5$	100.0%	98.9%
Max. and min. transmission	0.265 and 0.112	0.4306 and 0.1932
Data $I > 2\sigma(I)$/restraints/parameters	4067/3/280	3975/6/263
Goodness-of-fit on F^2	1.011	1.032
Final R indices [$I > 2\sigma(I)$]	$R_1 = 0.0209$ w$R_2 = 0.0492$	$R_1 = 0.0196$ w$R_2 = 0.0473$
R indices (all data)	$R_1 = 0.0281$ w$R_2 = 0.0519$	$R_1 = 0.0264$ w$R_2 = 0.0499$
Largest diff. peak and hole (e Å^{-3})	0.560 and −0.704	0.543 and −0.732
	3	**4**
Empirical formula	$C_{32}H_{40}N_4O_{14}PbS$	$C_{36}H_{32}N_4O_{12}Pb_2S_2$
Formula weight	943.93	1191.16
Temperature (K)	120(2)	296(2)
Wavelength (Å)	0.71073	0.71073
Crystal system	Triclinic	Triclinic
Space group	P-1	P-1
a (Å)	11.6178(9)	9.1111(9)
b (Å)	13.1516(10)	9.3230(9)
c (Å)	13.2212(10)	11.2213(11)
α (°)	64.0230(10)	91.5720(10)
β (°)	88.3840(10)	95.9980(10)
γ (°)	88.9160(10)	91.2770(10)
Volume [Å^3]	1815.2(2)	947.29(16)
Z	2	1
D_{Calc} [Mg/m^3]	1.727	2.088
Absorption coeff. [mm^{-1}]	4.777	9.054
F (000)	940	568
θ Range for data collection (°)	1.72–27.68	1.83–27.58
Index ranges	$-15 \leqslant h \leqslant 15$ $-17 \leqslant k \leqslant 16$ $-17 \leqslant l \leqslant 15$	$-11 \leqslant h \leqslant 11$ $-12 \leqslant k \leqslant 11$ $-14 \leqslant l \leqslant 14$
Reflections collected	16,117	8351
Unique (R_{int})	8306 [$R_{(int)} = 0.0223$]	4272 [$R_{(int)} = 0.0279$]

(*Continued*)

Table 1. (*Continued*).

	3	**4**
Completeness to $\theta = 27.5$	97.6%	97.4%
Max. and min. transmission	0.751 and 0.638	0.337 and 0.131
Data $I > 2\sigma(I)$/restraints/parameters	7271/ 0/471	3870/3/262
Goodness-of-fit on F^2	1.034	1.123
Final R indices [$I > 2\sigma(I)$]	$R_1 = 0.0291$	$R_1 = 0.0274$
	$wR_2 = 0.0776$	$wR_2 = 0.0722$
R indices (all data)	$R_1 = 0.0363$	$R_1 = 0.0323$
	$wR_2 = 0.0845$	$wR_2 = 0.0825$
Largest diff. peak and hole (e Å^{-3})	0.818 and −0.546	0.572 and −0.824

synthesized under ambient conditions. The aqueous mixture of Pb(II) salt and the corresponding acid in the presence of auxiliary chelating ligand, bipy/phen, usually first results in precipitation. Crystals are formed by slow evaporation of the solvent. NaOH was used to neutralize the acid. The molar ratio of acid : NaOH is very important for growth of single crystals. The molar ratios of acid : NaOH (1:1 for **1**, 1:0.5 for **2**, 1:0 for **3**, and 2:1 for **4**) were used when we synthesized the complexes (scheme 1). Otherwise, polycrystals or cotton-like solids were obtained. All carboxylate and sulfonate groups in **1–4** were deprotonated as supported by FT-IR spectral data and the results of crystallographic analysis (see below). There are differences in the coordination modes of the two methyl-substituted isomeric ligands (scheme 2), which exert influence on the crystalline architectures as described below.

3.2. *Crystal structure descriptions*

3.2.1. Structure description of [Pb(phen)(4-msba)(H_2O)] (1). X-ray crystallographic analysis reveals one Pb(II), one 4-msba, one phen, and one coordinated water in the asymmetrical unit of **1**. Each Pb(II) is chelated by two nitrogens of phen, four oxygens from two different 4-msba ligands, and one oxygen from water, resulting in seven-coordinate geometry with [PbN_2O_5] chromophore (figure 1(A)).

Valuable knowledge is obtained from studies on the Pb(II) $6s^2$ lone pair [46–48]. A stereochemically active $6s^2$ lone pair of electrons of Pb(II) plays an important role in the structure. The $6s^2$ lone pair is termed inactive if it has no steric effects and Pb(II) exhibits holodirected geometry with all of the Pb(II)–L bonds of similar lengths. However, an active $6s^2$ lone pair leads to very long Pb(II)–L bonds at the site occupied by the lone pair, and a shortening of the Pb(II)–L bond opposite to this site. The Pb–N bond distances for complexes with an inactive $6s^2$ lone pair usually fall in the range of 2.62–2.88 Å [49]. The Pb–N distances in **1** [Pb1–N1 2.499(3), Pb1–N2 2.594(3) å] are shorter and located at the site opposite to the lone pair. The Pb–N distances fall within the ranges usually observed in Pb(II) complexes containing a phen with an active lone pair [26, 27]. The distances of Pb–$O_{sulfonate}$ and Pb–O_{water} are longer than those of Pb–$O_{carboxylate}$ (table S1). Therefore, the presence of an active $6s^2$ lone pair opposite to phen and near to Pb–$O_{sulfonate}$ is confirmed. Thus, the chromophore [PbN_2O_5] exhibits hemidirected geometry.

The sulfonate group S1O3O4O5 from 4-msba exhibits the *syn-skew* bridging conformation in **1** results in the formation of a centrosymmetric sulfonate-bridged dinuclear

eight-membered (Pb1O1S1O2Pb1aO1aS1aO2a) secondary building unit (SBU) $[Pb_2(SO_3)_2(phen)_2]$. The distance between coordinated O2 and H18 attached to C18 in phen is 2.523 Å, which indicates the existence of a C18-H18 O2 hydrogen bond (table S2), which plays an important role in formation of the SBU in **1**. There are no Pb Pb contacts within the SBU (Pb1 Pb1#2: 4.877 Å). The carboxylate O1C1O2 shows bidentate chelating coordination. Thus, 4-msba affords the chelating-bridging $(k^1\text{-}k^1\text{-}\mu_2)\text{-}(k^2)\text{-}\mu_3$ coordination mode (scheme 2) and bridges adjacent SBUs into a 2D network. From the topological point of view, this network can be simplified by considering the SBUs as 4-connected nodes and 4-msba as linkers. Thus, **1** is simplified as a 2D (4,4)-network (figure 1(B)).

Hydrogen bonds exist between coordinated water O1 W and coordinated oxygen O5 in the adjacent layer [O1 W-H1W2…O5 2.830(5) å]. Thus, an extended 3D supramolecular network is formed (figure 1(C)).

3.2.2. Structure description of [Pb(bipy)(4-msba)(H_2O)]·H_2O (2). Complex **2** shows a similar structure to **1**. In the asymmetrical unit, there are one Pb(II), one 4-msba, one bipy, one coordinated water, and one lattice water. Each Pb(II) is seven-coordinate by two

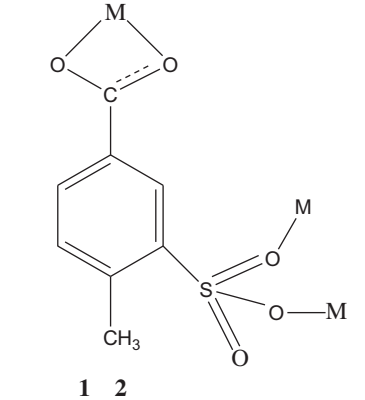

1 2

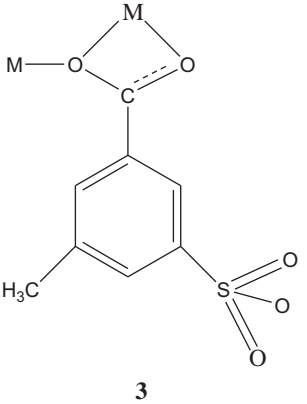

3

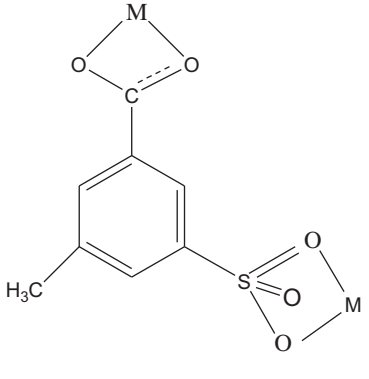

4

Scheme 2. Coordination modes of the substituted ligands in **1–4**.

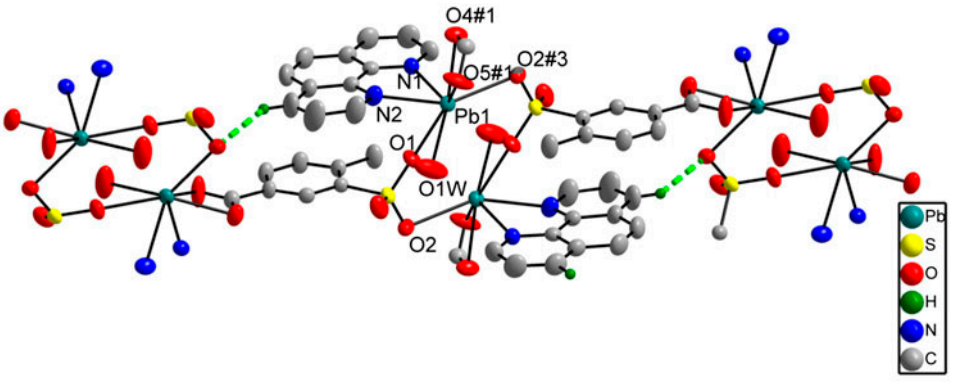

Figure 1A. View of the coordination environment of Pb(II), the coordination mode of 4-msba, the SBU in **1**, where hydrogen bonds are represented by dashed lines (#1: $-x+1$, $y+1/2$, $-z+1/2$; #3: $1-x$, $1-y$, $1-z$).

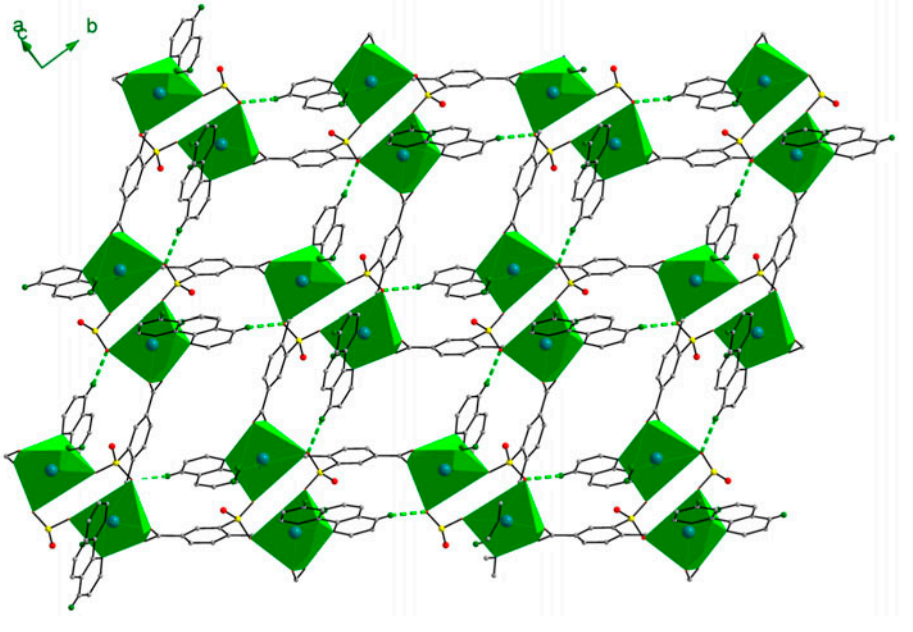

Figure 1B. 2D network with (4,4) topology.

bipyridine nitrogens, one oxygen from coordinated water, and two oxygens from carboxylate in one 4-msba and two oxygens from one sulfonate in the other 4-msba to furnish a hemidirected $[PbN_2O_5]$ geometry (figure 2(A)). The bond distances of the carboxylate and sulfonate in 4-msba are almost the same as those in **1** (table S1). Pb–$O_{carboxylate}$ distances are greatly shorter than those of Pb–$O_{sulfonate}$. The Pb–N distances [Pb1–N1 2.539(3), Pb1–N2 2.491(3) å] in **2** are shorter and locate in the site opposite to the $6s^2$ lone pair. These Pb–N distances fall within the ranges usually observed in Pb(II) complexes containing a bipy ligand with an active $6s^2$ lone pair [28] and slightly longer than those containing a substituted bipy [50]. Therefore, the $6s^2$ lone active pair in Pb(II) is confirmed.

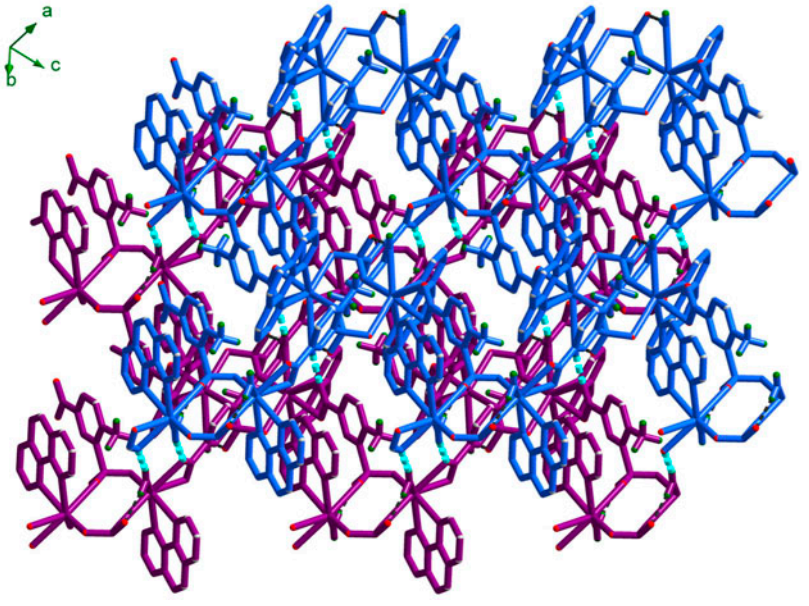

Figure 1C. 3D supramolecular network, where the green dashed lines represent hydrogen bonds (see http://dx.doi.org/10.1080/00206814.2013.815747 for color version).

The sulfonate group S1O3O4O5 from 4-msba ligand exhibits the same *syn-skew* bridging conformation as in **1**, resulting in centrosymmetric sulfonate-bridged dinuclear eight-membered [Pb1O5S1O3Pb1aO5aS1aO3a] SBU $[Pb_2(SO_3)_2(bipy)_2]$ (figure 2(A)). The hydrogen bonds C1–H1…O5 and C8–H8…O5 [2.696(2), 2.708(5) Å] may partly be responsible for formation of the SBU in **2**. The Pb Pb1#2 separation in each SBU is 4.773 (5) Å, which is longer than the sum of van der Waals radii (4.6 Å), indicating there are no Pb Pb contacts. The carboxylate O1C1O2 shows the same chelating coordination mode to Pb(II) as in **1**. So, 4-msba in **2** also affords the $(k^1\text{-}k^1\text{-}\mu_2)\text{-}(k^2)\text{-}\mu_3$ coordination (scheme 2) and bridges adjacent SBUs into a 2D (4,4)-framework (figure 2(B)).

Coordinated water O1 W is further hydrogen-bonded to coordinated carboxylate O2 in the adjacent layer [O1 W…O2 2.905(4) å] (table S2). Thus, a 3D supramolecular framework with 1D microporous channels is formed (figure 2(C)). Hydrogen-bonding plays an important role in the solid-state 3D supramolecular framework structure.

3.2.3. Structure description of $[Pb(5\text{-msba})(phen)_2]\cdot 9H_2O$ (3). X-ray crystallography shows each Pb(II) in **3** is seven-coordinate by four nitrogens from a pair of phen ligands and three oxygens from two carboxylates from two different 5-msba ligands, in which six bond lengths are relatively shorter and one longer (dashed line in figure 3(A)), termed as "primary" and "secondary" bonds, respectively (table S1) [51]. Secondary bonds are often overlooked and such bonds have been accepted as bonding [52]. The shorter distances of Pb1–O5 [2.489(3) å] and Pb1–N3 [2.510(3) å] compared with those of Pb1–N1 [2.713(3) å] and Pb1–O5#1 [3.140(4) å] reveal that the $6s^2$ lone pair on Pb(II) is active. The lone pair locates opposite to N3 and O5 and near to N1 and O5#1. The carboxylate group exhibits bidentate chelating-bridging $k^2\text{-}k^1\text{-}\mu_2$ coordination, while the sulfonate does not take part in coordination. The bond distances of $Pb\text{–}O_{carboxylate}$ in **3** are in the typical range of

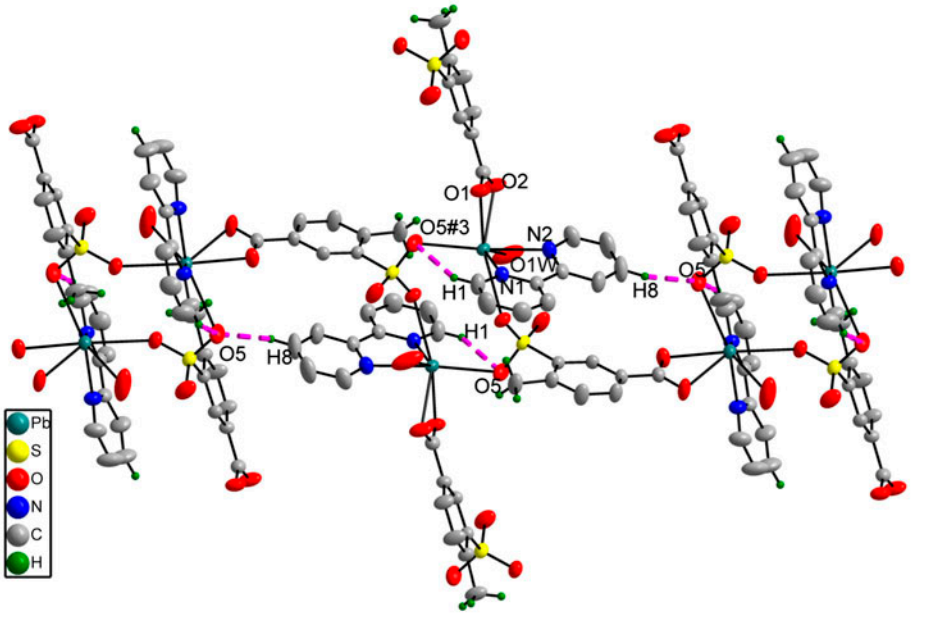

Figure 2A. The coordination environment of Pb(II), the coordination mode of 4-msba, and the SBU $[Pb_2(SO_3)_2(bipy)_2]$ in **2**. (Symmetry operator: #1 $-x+1/2$, $y-1/2$, $-z+1/2$; #3 $1/2+x$, $3/2-y$, $1/2+z$.)

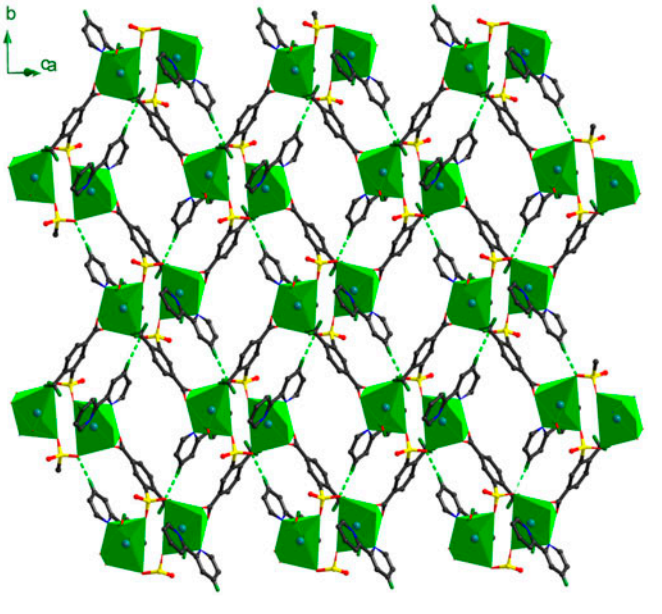

Figure 2B. 2D (4,4)-network.

2.489–2.516 Å. However, the bond length of Pb1–O5#1 is longer than the sum of the ionic radii but significantly shorter than the sum of the van der Waals radii (3.54 Å) [53], which can be explained by the presence of an active lone pair.

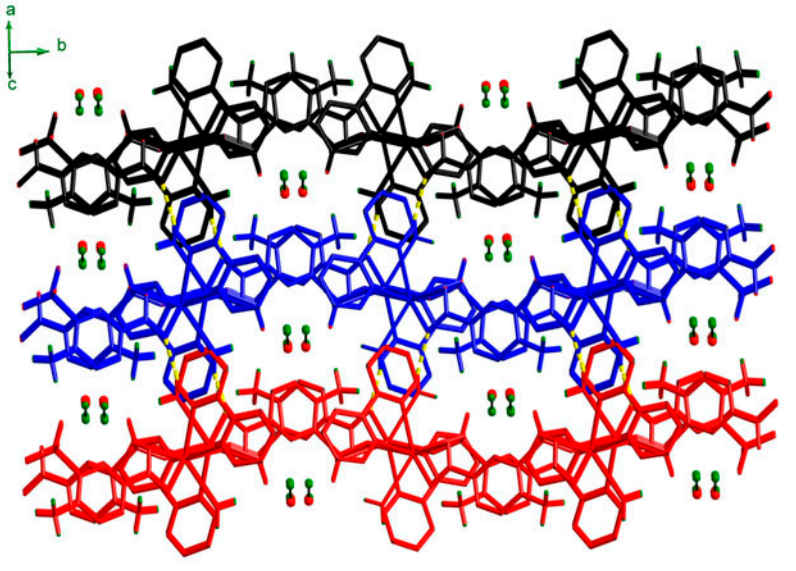

Figure 2C. 3D supramolecular framework formed through interlayer hydrogen bonds (yellow dashed lines) (see http://dx.doi.org/10.1080/00206814.2013.815747 for color version).

The weak secondary bond Pb1–O5#1 further leads to formation of a centrosymmetric dinuclear unit (figure 3(A)). In the dinuclear unit, the dihedral angle between the aromatic ring of 5-msba and phen is 5.68°, revealing that these two planes are almost parallel. Each asymmetric unit contains nine lattice waters.

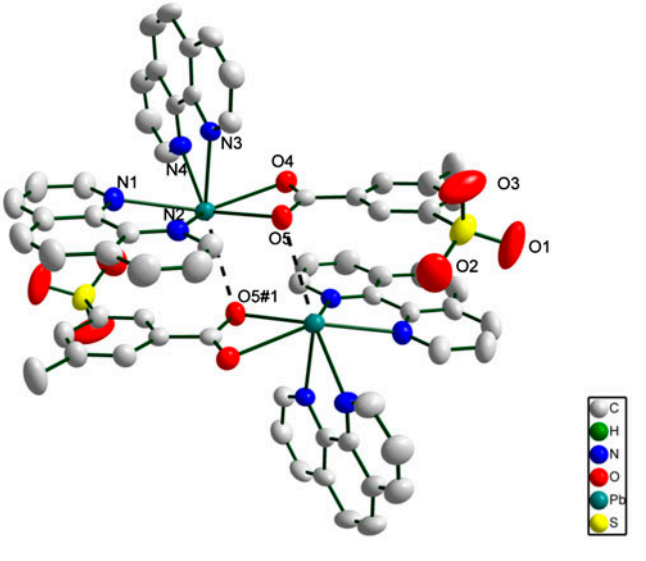

Figure 3A. The coordination environment of Pb(II) and the coordination mode of 5-msba in **3** (#1: $1-x$ $1-y$ $1-z$).

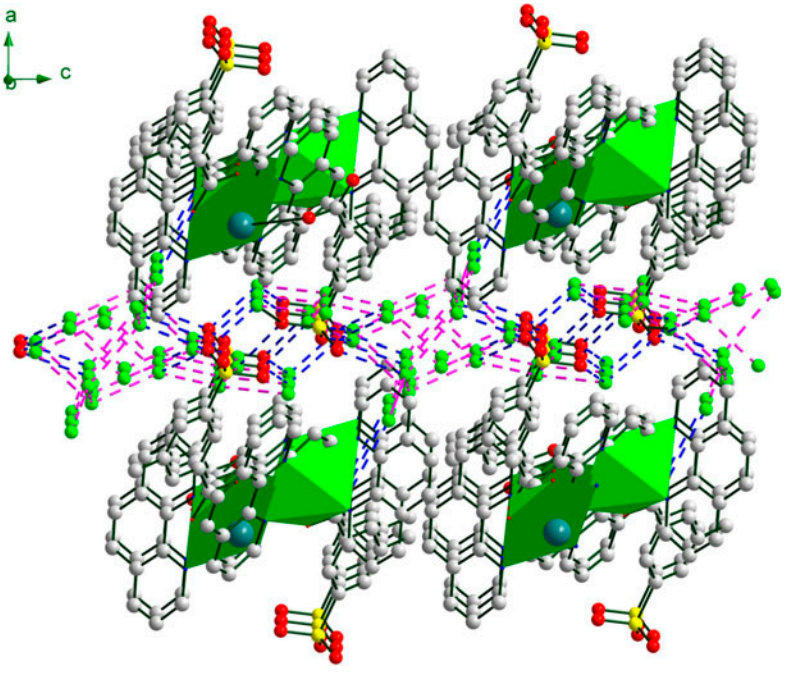

Figure 3B. 3D supramolecular network with hydrophilic gaps where the water tapes reside. The water–water and water-carboxylate/sulfonate hydrogen bonds are denoted by pink and blue dashed lines, respectively. (The green balls represent lattice waters) (see http://dx.doi.org/10.1080/00206814.2013.815747 for color version).

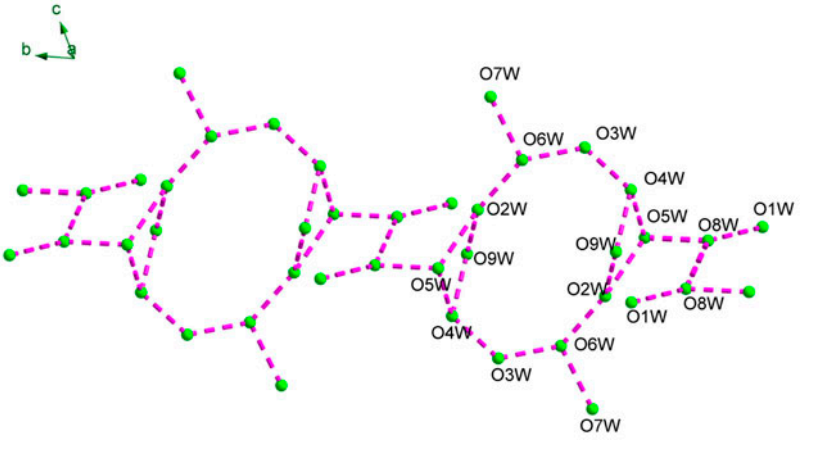

Figure 3C. 1D hydrogen-bonded water tape T4(3)4(3)10(3)A4.

Investigations on small hydrogen-bonded water clusters have been subject of both theoretical and experimental research, as their structural information is the first step toward understanding the behavior of bulk water [54–57]. For example, both the water dimer and trimer have been found in a Mn complex [58]. 1D water tapes with $(H_2O)_{16}$ cluster units have been found in a Co complex [59]. A 1D metal–water chain and a 2D water–sulfate

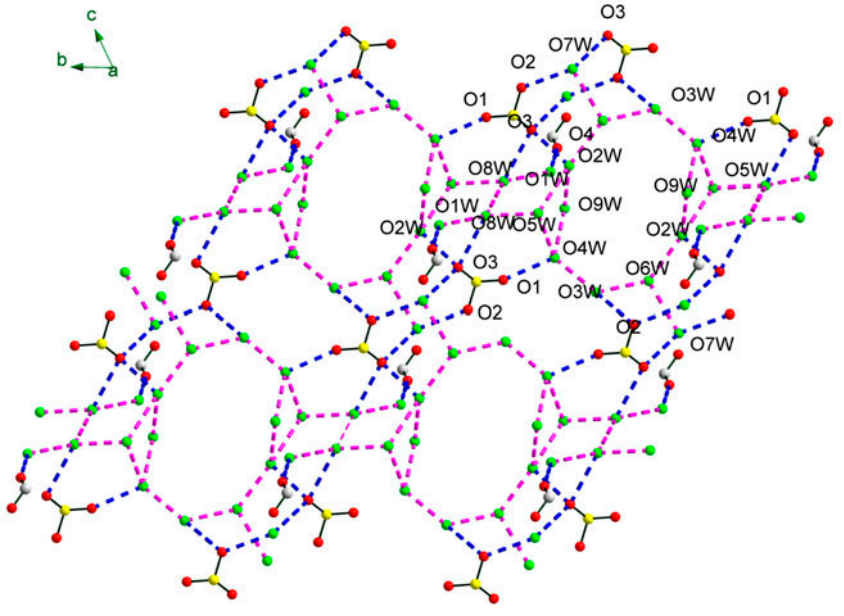

Figure 3D. Hydrogen-bonded layer and the coordination environment of water.

layer containing cyclic water octamers has been found in a tetranuclear Cu(II) complex [60]. In **3**, nine lattice waters and their centrosymmetric ones together assemble into a water cluster $(H_2O)_{18}$, which consists of an acyclic tetrameric water cluster and a $(H_2O)_{14}$ cluster containing a dodecameric tricyclic water ring with two pendent symmetric waters (figure 3(C)). The configuration of the $(H_2O)_{18}$ water cluster presented here is quite different from that with a turbine-type conformation composed of a water hexamer and six dangling $(H_2O)_2$ units in a reported Mn(III) complex [61]. The $(H_2O)_{14}$ cluster and acyclic tetrameric water cluster arrange alternatively, resulting in formation of a water tape pattern T4(3)4(3)10(3)A4. The Ow…Ow distances range from 2.705 to 3.173 Å with an average distance of 2.895 Å, which is comparable to the average O O contact of *ca*. 2.85 Å found in liquid water [62] but longer than the corresponding value of 2.759 Å in hexagonal ice (I_h) [63].

The water tapes are located in hydrophilic gaps. There are hydrogen-bonding interactions between the water tapes and uncoordinated sulfonate oxygens (O1, O2, O3), and coordinated carboxylate oxygen (O4) (figure 3(D)) resulting in an extended 3D supramolecular network (figure 3(B)). Thus, the hydrogen-bonded water tape serves as glue to link adjacent dinuclear units into a 3D supramolecular network.

3.2.4. Structure description of $[Pb_2(5\text{-msba})_2(bipy)_2(H_2O)_2]$ (4). Complex **4** exhibits a centrosymmetric dinuclear structure. Each symmetric unit contains two Pb(II) ions, two 5-msba, two coordinated waters, and two bipy. Each Pb(II) is seven-coordinate with one bipy, one oxygen from coordinated water, two oxygens from carboxylate, and two oxygens from sulfonates of two different 5-msba. Six bond lengths are relatively shorter ("primary" bonds) and one longer ("secondary" bond) (figure 4(A); table S1) [51].

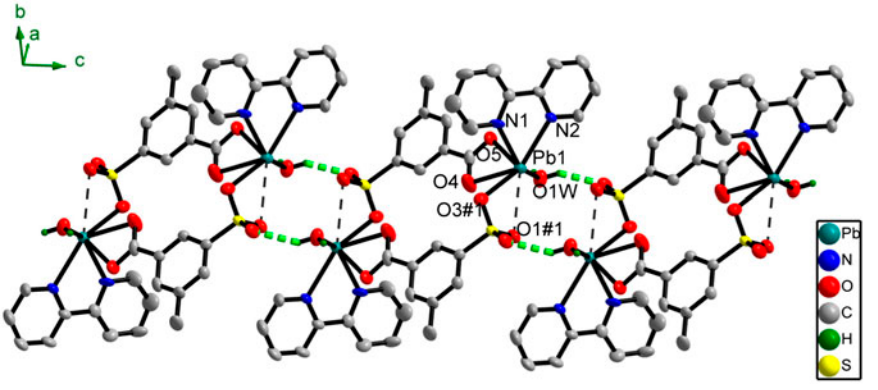

Figure 4A. The coordination geometry of Pb(II) and the supramolecular ladder-like chain formed through the $R_2^2(12)$ membered ring in **4** (#1: $1-x$, $1-y$, $1-z$).

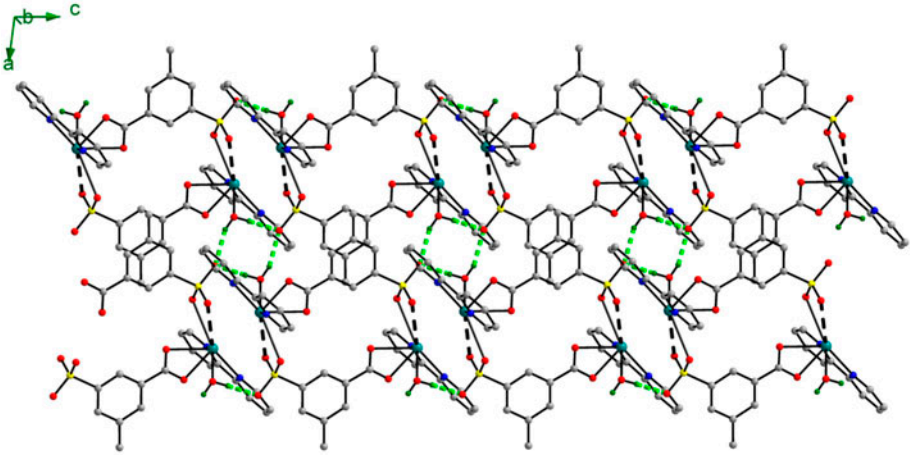

Figure 4B. H-bonded supramolecular layer consisting of two kinds of supramolecularrings.

Both sulfonate and carboxylate exhibit bidentate chelating coordination. Pb–$O_{sulfonate}$ distances are longer than those of Pb–$O_{carboxylate}$, indicating that carboxylate has stronger coordination to Pb(II) than sulfonate. The Pb1–O1 bond length [3.061(4) å] is longer than the sum of the ionic radii but significantly shorter than the sum of the van der Waals radii (3.54 Å) [53], which can be explained by the presence of an active lone pair in the proximity of the sulfonate.

The Pb–N distances in **4** are shorter and locate in the site opposite to the $6s^2$ lone pair. These Pb–N distances fall within the ranges usually observed in hemidirected Pb(II) complexes containing bipy with an active lone pair [28]. Therefore, the presence of an active lone pair is confirmed.

Hydrogen bonds exist between coordinated water O1 W and uncoordinated sulfonate oxygen (O1 and O2) in the lattice. Dinuclear units are linked through a 12-membered hydrogen-bonded supramolecular metallamacrocyclic ring $R_2^2(12)$ into a ladder-like chain (figure 4(A)).

The chains are further linked through eight-membered $R^2_4(8)$ hydrogen-bonded rings (O1w···O2 2.829, O1w···O2 2.830, O1w···O1 3.139 Å) (table S2). Thus, an extended 2D supramolecular network is formed (figure 4(B)).

3.3. *Coordination geometry of lead(II)*

The stereochemical activity of the $6s^2$ lone electron pair in Pb(II) is an interesting and ubiquitous issue. Shimoni–Livny and co-workers classify the geometries of Pb(II) in its complexes as holo and hemidirected [46]. Holodirected refers to lead(II) complexes in which the bonds to ligands are placed throughout the surface of the encompassing globe, while hemidirected refers to cases in which the bonds to ligands are directed throughout only part of an encompassing globe. It has been found through *ab initio* molecular orbital studies of Pb(II) complexes in gas phase that a hemidirected geometry occurs if the ligands are hard, the ligand coordination number is low, and attractive interactions exist between the ligands [46, 64]. In **1–4**, the coordination number of Pb(II) is seven. The $6s^2$ lone electron pairs are clearly active. Thus, coordination spheres of Pb(II) in **1–4** are all hemidirected (figure 5).

3.4. *Discussion of the structures*

The dimensionalities decrease from 2D for **1** and **2** with 4-msba to 0D dimeric species for **3** and **4** with 5-msba. Consequently, there is a clear relationship between the positions of the methyl and dimensionalities of the structures of **1–4** (scheme 1).

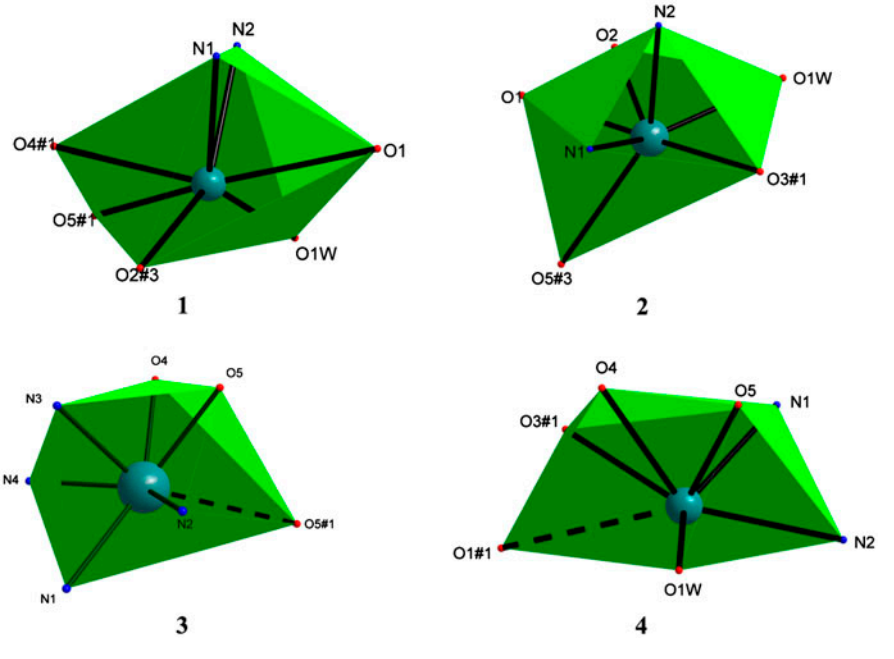

Figure 5. Polyhedral representation of the hemidirected lead(II) in **1–4**.

Although **1** and **2** have the same structural topology, the packing diagrams are different. The 3D supramolecular framework of **2** has 1D channels occupied by lattice waters, but the framework of **1** does not.

The SBU in **4** has a different structure than those in **1** and **2**. In the SBUs of **1** and **2**, the bipy and phen ligands are almost parallel with the aromatic ring of 4-msba, resulting in the formation of a 2D (4,4)-net (figures 1 and 2). The different positions of CH_3 in the aromatic rings may be responsible for the different configurations of SBUs, and consequently affect the final architectures.

3.5. *FT-IR Spectra and thermal stability*

IR spectral data show features attributable to carboxylate and sulfonate stretching vibrations of **1**, **2**, **3A**, and **4**. The absence of bands at 1680–1760 cm^{-1} indicates complete deprotonation of the corresponding acid in all compounds. IR results are commonly employed to distinguish coordination modes of carboxylates. A correlation of the carboxylate coordination mode to metal ions is usually made by examining the difference $\Delta\nu(COO) = \nu_{as}(COO) - \nu_s(COO)$ of the complexes [65]. The vibrations of $\nu_{as}(COO)$ and $\nu_s(COO)$ are at 1582 and 1396 cm^{-1} for **1**, 1630 and 1522 cm^{-1} for **2**, 1533 and 1385 cm^{-1} for **3A**, and 1545 and 1392 cm^{-1} for **4**. The $\Delta\nu[\nu_{as(C=O)} - \nu_{s(C=O)}]$ are all smaller than 200 cm^{-1}, indicating that the carboxylates in all the complexes function in chelating bidentate motifs [65]. In all these cases, the results of X-ray analysis allow unambiguous assignment of the binding modes of carboxylate. The broad band at 3600–3200 cm^{-1} corresponds to vibration of water in the complexes. The FT-IR spectra contain characteristic peak of sulfonate: 1231 cm^{-1} for **1**, 1176 cm^{-1} for **2**, 1164 cm^{-1} for **3A**, and 1207 cm^{-1} for **4**, respectively [65].

To study the thermal stability of the complexes, thermogravimetric analysis (TG) was performed on all samples under flowing N_2 (figure S1). TGA of **1** suggests that the first weight loss (2.79%) from 42–118 °C corresponds to loss of water (Calcd 2.90%). Complex

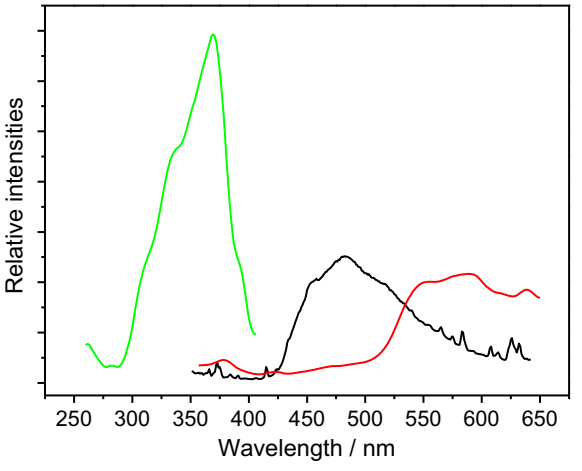

Figure 6. Emission spectra of **1** (red), **2** (black) and H_2(4-msba) (green) in the solid state (λ_{ex} = 337, 332, 213 nm, respectively) at room temperature (see http://dx.doi.org/10.1080/00206814.2013.815747 for color version).

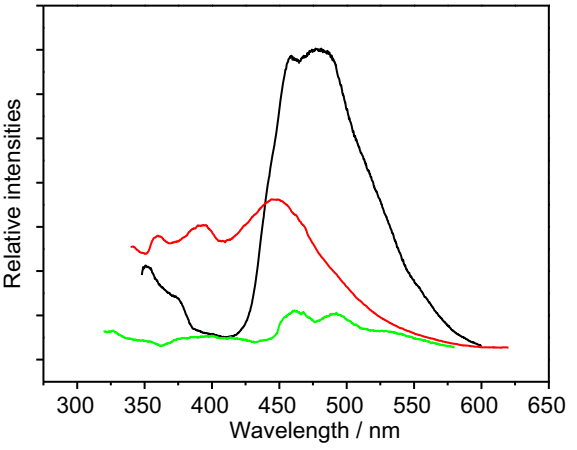

Figure 7. Emission spectra of H_2(5-msba) (red), [Pb(5-msba)(phen)$_2$]·2H_2O (**3A**) (green), and [Pb_2(5-msba)$_2$(2,2′-bipy)$_2$(H_2O)$_2$] (**4**) (black) in the solid state at room temperature. The corresponding excitation wavelengths, λ_{ex} are 326, 300, and 328 nm, respectively (see http://dx.doi.org/10.1080/00206814.2013.815747 for color version).

2 exhibits a weight loss of 5.29% at 41–151 °C, corresponding to loss of all waters (Calcd 5.81%). The weight loss beginning at 283 °C corresponds to the decomposition of the framework. The total weight loss of 49.56% from 42–800 °C is in agreement with the weight loss calculated for loss of all moieties leading to formation of $PbSO_4$ as final residuals (Calcd 49.38%).

For [Pb(msba)(phen)$_2$]·2H_2O (**3A**), the first weight loss of 4.32% (Calcd 4.40%) from 50 to 125 °C corresponds to removal of two lattice waters, which reveals that the partly desolvated **3A** results from loss of seven waters in [Pb(msba)(phen)$_2$]·9H_2O (**3**). The second step begins at 250 °C.

In **4**, the weight decrease of 3.13% from 100 to 129 °C corresponds to loss of water (Calcd 3.02%). The second decomposition begins from 289 °C followed by a long tail.

3.6. *Fluorescence properties in the solid state*

To study the fluorescent intensities of **1–4**, solid state fluorescent emission spectra were determined at room temperature. Excitation of **1**, **2**, **3A**, and **4** at 337, 332, 300, and 328 nm, respectively, leads to different fluorescent emissions with the maximum emission centered at 575, 482, 460, and 477 nm, respectively (figures 6 and 7). To understand the origin of these emission bands, fluorescence spectra of H_2(4-msba), H_2(5-msba), 2,2′-bipy, and phen have also been measured. The two isomeric acids, H_2(4-msba) and H_2(5-msba), exhibit maximum emission at 357 nm (λ_{ex} = 213 nm) and 448 nm (λ_{ex} = 326 nm), respectively. The 2,2′-bipy and phen show maximum emission at 400 and 392 nm (λ_{ex} = 300 nm), respectively (figure S2). So, all the maximum emissions for **1**, **2**, **3A**, and **4** are red shifted compared to those for both the corresponding free acid and 2,2′-bipy or phen. The red shifts are caused by either the coordination of the substituted acids and 2,2′-bipy, or phen or an interaction between ligands perturbed by lead(II). These complexes exhibit multiple peaks due to the mixed ligands (one substituted acid ligand and neutral chelating ligands, bipy/phen) contained in the complexes. The coexistence of chelating and bridging ligands in complexes leads to ligand-to-ligand charge transfer [66].

4. Conclusion

The study presents a strategy for tuning network architectures through changing the positions of the substituent and broadens the use of methyl-substituted 3-sulfobenzoic acid as spacers for construction of Pb(II) supramolecular complexes. Structural characterizations of these complexes give valuable information. (1) Assemblies of four complexes generate two 2D (4,4)-networks with 4-msba and two dimeric species with 5-msba. These structures are largely controlled by the positions of the methyl. (2) Three different coordination modes of the substituted acid ligands have been found. The bipy/phen have great influence on coordination of 5-msba, but have no influence on coordination of 4-msba. (3) The $6s^2$ lone pairs of Pb(II) are all stereochemically active. (4) Compounds **1**, **2**, and **4** are solvent-poor, while **3** is relatively solvent-rich due to the existence of the hydrophilic gaps between the supramolecular layers. (5) The diverse structures lead to diverse fluorescent properties, important for synthesis of desired frameworks with specific usage. This work enriches the Pb(II) coordination chemistry.

Supplementary material

Crystallographic data have been deposited with the Cambridge Crystallographic Data Center with Nos. 679921 (**1**), 679920 (**2**), 766587 (**3**), and 766588 (**4**). Copies of the data can be obtained free of charge via the Internet at http://www.ccdc.cam.ac.uk/conts/retrieving.html.

Acknowledgments

The Natural Science Foundation of Jiangsu Province (BK2012680), the Priority Academic Program Development of Jiangsu Higher Education Institutions (PAPD), the Jiangsu Government Scholarship for Overseas Studies, and the foundation from Key Laboratory of Environmental Material and Environmental Engineering of Jiangsu Province are gratefully acknowledged.

References

[1] D.J. Tranchemontagne, J.L. Mendoza-Cortés, M. O'Keeffe, O.M. Yaghi. *Chem. Soc. Rev.*, **38**, 1257 (2009).
[2] G.-X. Liu, Y.-Q. Huang, Q. Chu, T. Okamura, W.-Y. Sun, H. Liang, N. Ueyama. *Cryst. Growth Des.*, **8**, 3233 (2008).
[3] Z.-Z. Lu, R. Zhang, Y.-Z. Li, Z.-J. Guo, H.-G. Zheng. *J. Am. Chem. Soc.*, **133**, 4172 (2011).
[4] J. An, S.J. Geib, N.L. Rosi. *J. Am. Chem. Soc.*, **132**, 38 (2010).
[5] J.M. Lehn. *Supramolecular Chemistry: Concepts Perspect.*, VCH, New York (1995).
[6] A. Morsali, M.Y. Masoumi. *Coord. Chem. Rev.*, **253**, 1882 (2009).
[7] Y. Liu, X. Xu, F.K. Zheng, Y. Cui. *Angew. Chem. Int. Ed.*, **47**, 4538 (2008).
[8] J.P. Zhang, X.M. Chen. *J. Am. Chem. Soc.*, **130**, 6010 (2008).
[9] D. Guo, K.-L. Pang, C.-Y. Duan, C. He, Q.-J. Meng. *Inorg. Chem.*, **41**, 5978 (2002).
[10] A.M. Beatty. *Coord. Chem. Rev.*, **246**, 131 (2003).
[11] M. Yoshizawa, M. Nagao, K. Umemoto, K. Biradha, M. Fujita, S. Sakamoto, K. Yamaguchi. *Chem. Commun.*, **1808**, (2003).
[12] X.-P. Li, J.-Y. Zhang, M. Pan, S.-R. Zheng, Y. Liu, C.-Y. Su. *Inorg. Chem.*, **46**, 4617 (2007).
[13] D.F. Sava, V. Kravtsov, J. Eckert, J.F. Eubank, F. Nouar, M. Eddaoudi. *J. Am. Chem. Soc.*, **131**, 10394 (2009).
[14] M. Oh, G.B. Carpenter, D.A. Sweigart. *Organometallics*, **22**, 2364 (2003).
[15] M. Du, Z.H. Zhang, Y.P. You, X.J. Zhao. *CrystEngCommun.*, **10**, 306 (2008).

[16] H. Ren, T.Y. Song, J.N. Xu, S.B. Jing, Y. Yu, P. Zhang, L.-R. Zhang. *Cryst. Growth Des.*, **9**, 105 (2009).
[17] F. Dai, H. He, D. Gao, F. Ye, X. Qiu, D. Sun. *CrystEngCommun.*, **11**, 2516 (2009).
[18] D.-S. Zhou, F.-K. Wang, S.-Y. Yang, Z.-X. Xie, R.-B. Huang. *CrystEngCommun.*, **11**, 2548 (2009).
[19] Y.Q. Xu, D.Q. Yuan, L. Han, E. Ma, M.Y. Wu, Z.Z. Lin, M.C. Hong. *Eur. J. Inorg. Chem.*, **2054**, (2005).
[20] X.-J. Li, R. Cao, Z.-G. Cuo, J. Lü. *Chem. Commun.*, **1938**, (2006).
[21] Y.H. Yeom, Y. Kim, K. Seff. *Microporous Mesoporous Mater.*, **28**, 103 (1999).
[22] (a) Y.H. Yeom, Y. Kim, K. Seff. *J. Phys. Chem.*, **B101**, 5314 (1997); (b) J. Yang, J.F. Ma, Y.Y. Liu, J.C. Ma, S.R. Batten. *Inorg. Chem.*, **46**, 6542 (2007).
[23] Y.H. Zhao, H.B. Xu, Y.M. Fu, K.Z. Shao, S.Y. Yang, Z.M. Su, X.R. Hao, D.X. Zhu, E.B. Wang. *Cryst. Growth Des.*, **8**, 3566 (2008).
[24] J. Yang, J.F. Ma, Y.Y. Liu, J.C. Ma, S.R. Batten. *Cryst. Growth Des.*, **9**, 1894 (2009).
[25] J. Yang, G.D. Li, J.J. Cao, Q. Yue, G.H. Li, J.S. Chen. *Chem. Eur. J.*, **13**, 3248 (2007).
[26] S.-R. Fan, L.-G. Zhu. *Inorg. Chem.*, **45**, 7935 (2006).
[27] S.R. Fan, L.-G. Zhu. *Inorg. Chem.*, **46**, 6785 (2007).
[28] K.L. Zhang, Y. Chang, C.-T. Hou, G.-W. Diao, R. Wu, S.W. Ng. *CrystEngCommun.*, **12**, 1194 (2010).
[29] H. Sadeghzadeh, A. Morsali, V.T. Yilmaz, O. Buyukgungor. *J. Coord. Chem.*, **63**, 3423 (2010).
[30] F. Marandi, V. Safarifard, A. Morsali, H.-K. Fun. *J. Coord. Chem.*, **64**, 3781 (2011).
[31] L. Hashemi, A. Morsali, H.-K. Fun. *J. Coord. Chem.*, **64**, 4088 (2011).
[32] M.A.R. Dakers, M.N.S. Hill, J.C. Lockhart, D.J. Rushton. *J. Chem. Soc., Dalton Trans*., 209 (1994).
[33] A.K. Cheetham, G. Ferey, T. Loiseau. *Angew. Chem. Int. Ed.*, **38**, 3268 (1999).
[34] S. Ayyappan, G.D. Delgado, A.K. Cheetham, G. Ferey, C.N.R. Rao. *J. Chem. Soc., Dalton Trans*., 2905 (1999).
[35] B. Chen, S. Ma, F. Zapata, F.R. Fronczek, E.B. Lobkovsky, H.-C. Zhou. *Inorg. Chem.*, **46**, 1233 (2007).
[36] B. Ding, Y.Y. Liu, X.X. Wu, X.-J. Zhao, G.X. Du, E.-C. Yang, X.G. Wang. *Cryst. Growth Des.*, **9**, 4176 (2009).
[37] K.L. Zhang, F. Zhou, R. Wu, B. Yang, S.W. Ng. *Inorg. Chim. Acta*, **362**, 4255 (2009).
[38] Z. Su, Z.-B. Wang, W.-Y. Sun. *J. Coord. Chem.*, **64**, 170 (2011).
[39] Z. Wang, Q. Wei, G. Xie, Q. Yang, S. Chen, S. Gao. *J. Coord. Chem.*, **65**, 286 (2011).
[40] M.K. Samy, D. Engelhart, P.N. Basa, A.G. Sykes. *J. Coord. Chem.*, **63**, 2261 (2010).
[41] X.J. Li, R. Cao, Z.G. Guo, Y.F. Li, X.D. Zhu. *Polyhedron*, **26**, 3911 (2007).
[42] B.D. Chandler, D.T. Cramb, G.K.H. Shimizu. *J. Am. Chem. Soc.*, **128**, 10403 (2006).
[43] S.A. Dalrymple, G.K.H. Shimizu. *J. Am. Chem. Soc.*, **129**, 12114 (2007).
[44] D.J. Hoffart, S.A. Dalrymple, G.K.H. Shimizu. *Inorg. Chem.*, **44**, 8868 (2005).
[45] G.M. Sheldrick. *SHELXL 97. Programs for Crystal Structure Analysis (Release 97–2)*, University of Göttingen, Germany (1997).
[46] L. Shimoni-Livny, J.P. Glusker, C.W. Bock. *Inorg. Chem.*, **37**, 1853 (1998).
[47] C. Gourlaouen, O. Parisel. *Angew. Chem. Int. Ed.*, **46**, 553 (2007).
[48] R.D. Hancock, J.H. Reibenspies, H. Maumela. *Inorg. Chem.*, **43**, 2981 (2004).
[49] R.D. Hancock, M.S. Shaikjee, S.M. Dobson, J.C.A. Boeyens. *Inorg. Chim. Acta*, **154**, 229 (1988).
[50] F. Marandi, Z. Nikpey, M. Khosravi, S. Hosseini, H.-K. Fun, M. Hemamalini. *J. Coord. Chem.*, **64**, 3012 (2011).
[51] J.S. Magyar, T.C. Weng, C.M. Stern, D.F. Dye, B.W. Rous, J.C. Payne, B.M. Bridgewater, A. Mijovilovich, G. Parkin, J.M. Zaleski, J.E. Penner-Hahn, H.A. Godwin. *J. Am. Chem. Soc.*, **127**, 9495 (2005).
[52] S.H. Dale, M.R.J. Elsegood, S. Kainth. *Acta Crystallogr.*, **C60**, m76 (2004).
[53] A.J. Bondi. *Phys. Chem.*, **68**, 441 (1964).
[54] L. Infantes, S. Motherwell. *CrystEngCommun.*, **4**, 454 (2002).
[55] K. Liu, M.G. Brown, C. Carter, R.J. Saykally, J.K. Gregory, D.C. Clary. *Nature*, **381**, 501 (1996).
[56] K. Nauta, R.E. Miller. *Science*, **287**, 293 (2000).
[57] F. Zappa, S. Denifl, I. Mähr, A. Bacher, O. Echt, T.D. Märk, P. Scheier. *J. Am. Chem. Soc.*, **130**, 5573 (2008).
[58] K. Zhao, Y. Jiang, X. Qiu, J. Tian, X. Li. *J. Coord. Chem.*, **64**, 1375 (2011).
[59] Z. Li, L. Huang, P. Xi, H.Y. Liu, Y. Shi, G.Q. Xie, M. Xu, F.J. Chen, Z. Zeng. *J. Coord. Chem.*, **64**, 1885 (2011).
[60] Y.-N. Gong, C.-B. Liu, X.-H. Tang, A.-Q. Zhang. *J. Coord. Chem.*, **64**, 2761 (2011).
[61] C.-H. Li, K.-L. Huang, J.-M. Dou, Y.-N. Chi, Y.-Q. Xu, L. Shen, D.-Q. Wang, C.-W. Hu. *Cryst. Growth Des.*, **8**, 3141 (2008).
[62] D. Eisenberg, W. Kauzmann. *The Structure and Properties of Water*, Oxford University Press, Oxford (1969).
[63] N.H. Fletcher. *The Chemical Physics of Ice*, Cambridge University Press, Cambridge (1970).
[64] C.W. Watson, S.C. Parker. *J. Phys. Chem.*, **B103**, 1258 (1999).
[65] K. Nakamoto. *Infrared and Raman Spectra of Inorganic and Coordination Compounds*, Wiley, New York, NY (1997).
[66] A. Vogler, H. Kunkely. *Coord. Chem. Rev.*, **251**, 577 (2007).